Car-following model with relative-velocity effect and its experimental verification

Daisuke Shamoto,[1] Akiyasu Tomoeda,[2,3] Ryosuke Nishi,[1] and Katsuhiro Nishinari[3,4]

[1]*Department of Aeronautics and Astronautics, School of Engineering, The University of Tokyo, Hongo, Bunkyo-ku, Tokyo 113-8656, Japan*

[2]*Meiji Institute for Advanced Study of Mathematical Sciences, Meiji University, 1-1-1 Higashimita, Tamaku, Kawasaki 214-8571, Japan*

[3]*Research Center for Advanced Science and Technology, The University of Tokyo, Komaba 4-6-1, Meguro-ku, Tokyo 153-8904, Japan*

[4]*PRESTO, Japan Science and Technology Corporation, Komaba 4-6-1, Meguro-ku, Tokyo 153-8904, Japan*

(Received 16 February 2010; revised manuscript received 10 January 2011; published 11 April 2011)

In driving a vehicle, drivers respond to the changes of both the headway and the relative velocity to the vehicle in front. In this paper a new car-following model including these maneuvers is proposed. The acceleration of the model becomes infinite (has a singularity) when the distance between two vehicles is zero, and the asymmetry between the acceleration and the deceleration is incorporated in a nonlinear way. The model is simple but contains enough features of driving for reproducing real vehicle traffic. From the linear stability analysis, we confirm that the model shows the metastable homogeneous flow around the critical density, beyond which a traffic jam emerges. Moreover, we perform experiments to verify this model. From the data it is shown that the acceleration of a vehicle has a positive correlation with the relative velocity.

DOI: 10.1103/PhysRevE.83.046105 PACS number(s): 89.40.−a, 02.50.−r, 02.70.Uu, 45.70.Vn

I. INTRODUCTION

In the last several decades, the dynamics of traffic flow has been investigated by many scientists in physics and mathematics using the formalism of many-body systems of self-driven particles [1–5].

One of the interesting phenomena of traffic flow is the emergence of traffic congestion due to the instability of the homogeneous flow, which has been recently verified by the experiment conducted in a circuit [6]. Many researchers have tried, up to now, to establish a mathematical model which has this feature. Especially, a lot of car-following models have been suggested since the 1950s. They are formulated by focusing each driver's movement against its preceding vehicle. Some of them successfully show the formation of traffic congestion as the instability of the homogeneous flow. Gazis and co-workers [7,8] suggested a car-following model which can be written as

$$\frac{d}{dt}v_j(t+\tau) = \lambda \frac{v_j^m(t)}{h_j^l(t)}\Delta v_j(t), \tag{1}$$

where l and m are constants, λ is a positive constant parameter, which expresses the sensitivities of drivers, v_j is the velocity of the jth vehicle, and $h_j = x_{j+1} - x_j$ is the headway to the vehicle in front. Accordingly, x_j corresponds to the position of the jth vehicle. $\Delta v_j = v_{j+1} - v_j$ represents the relative velocity. We use this term as the difference between the velocity of the vehicle in front and that of the given vehicle. Thus $\Delta v_j < 0$ corresponds to the situation in which the $(j+1)$th vehicle is getting closer to the jth vehicle, and $\Delta v_j > 0$ corresponds to the counter situation. The acceleration of the jth vehicle is delayed for a reaction time τ. Since, according to Eq. (1), the acceleration depends on the vehicle in front, there is a critical problem that this model is not applicable for very low traffic densities. If the vehicle in front is very far (corresponding to $h_j \to \infty$), the acceleration of the jth vehicle is zero, regardless of the jth own velocity. This means that the velocity of the jth vehicle cannot be determined in very low traffic densities. Actually, in this case, drivers tend to accelerate to their desired velocity.

Newell [9] solved this problem by introducing a headway-dependent function, called the optimal velocity (OV) function. His model is described as

$$v_j(t+\tau) = V[h_j(t)], \tag{2}$$

where the OV function V is given as $V(h) = V_0\{1 - \exp[-\gamma(h-d)]/V_0\}$ with γ, V_0, and d parameters associated with characteristics of drivers. In this model, if the headway is large enough (corresponding to $h \to \infty$), the velocity converges to the desired velocity V_0. Although this model solved the problem of the applicability to very low traffic densities, another problem remains. This model assumes that the vehicle's velocity is adjusted by the headway to the vehicle in front with the delay τ. However, drivers adjust only the acceleration by putting on the accelerating or the braking pedals in real driving.

Helly [10,11] proposed another car-following model. This model combines two stimuli of a driver: keeping up the safe headway and following the leading vehicle to maintain his/her relative velocity equal to zero with time delay. However, as we discuss later, it is not consistent with experimental results if the two stimuli act linearly on the acceleration.

In the 1990s, Bando *et al.* [12] suggested another car-following model,

$$\frac{d}{dt}v_j = \frac{1}{\tau}[V(h_j) - v_j], \tag{3}$$

which can be obtained by the Taylor expansion of Eq. (2) in terms of τ. This model has been widely used by physicists because of its simplicity. In the model, traffic congestion is expressed as a limit cycle from the viewpoints of nonlinear dynamics [13]. For typical values of the parameters [12], crashes between successive vehicles are avoided if $\tau < 0.9$ sec. Moreover, in models (2) and (3), drivers respond to the stimuli, which is a function of only the headway. In real driving, drivers' responses are affected not only by the headway but also by the relative velocity, as a lot of studies show.

In more recent studies, some models that contain the relative velocity effect are proposed. In the intelligent driver model (IDM) [14], vehicles' acceleration is determined by their

 ©2011 American Physical Society

headway, their own velocity, and their relative velocity. The model consists of the linear combination of a relaxation term and a braking term. Relative velocity is taken into account in the braking term divided by two new parameters, i.e., the maximum acceleration and the comfortable deceleration. A verification of this model by using a car-following experiment with GPS satellites has shown that braking behaviors in the model does not coincide with experiments [15].

Another example is the full velocity difference model [16], which is formulated by linearly adding the relative velocity term to Eq. (3). However, the dependence of the relative velocity on the acceleration is not so simple but nonlinear in reality, as shown later. A similar model of linear dependence of the relative velocity is proposed in [17–19].

Note that the model in [17] has a singularity, which is given by the equation

$$\frac{d}{dt}v_j = A\left(1 - \frac{h_j^0}{h_j}\right) - \frac{Z^2(-\Delta v_j)}{2(h_j - D)} - kZ(v_j - v_{\mathrm{per}}) + \eta, \tag{4}$$

where the safety distance h_j^0 is written as $h_j^0 = v_j T + D$, the function Z is defined as $Z(x) = (x + |x|)/2$, the parameter η is a white-noise term and the other parameters A, D, v_{per}, and k are constant.

Although a lot of car-following models have been suggested for several decades, we are still far from reaching "the basic equation" for vehicle traffic. Therefore in this paper we first discuss the criteria that a realistic car-following model should satisfy. Then we propose a different car-following model that meets the criteria, and compare the model with experimental data in detail. The experimental data show the asymmetry between the acceleration and the deceleration not found in the previous experiments [20].

This paper is organized as follows. In Sec. II we discuss the important features of driving, and give the criteria which a car-following model should have. In Sec. III we propose a new car-following model, and analyze the linear stability of the homogeneous flow in Sec. IV. Results of simulations under the periodic boundary condition is given in Sec. V, and comparison between experimental data and the model is shown in Sec. VI. Finally, Sec. VII is devoted to the concluding discussions.

II. CRITERIA FOR REALISTIC CAR-FOLLOWING MODELS

We first discuss important properties that are required for realistic car-following models. From the brief historical review given in the previous section, we summarize the criteria in the following way:

(A) Drivers can adjust only their accelerations.

(B) Simulations must be stopped when two vehicles overlap with each other.

(C) The model should be experimentally accessible.

These three requirements are necessary and should apply to realistic models. Let us explain the criteria in detail.

(A) Every driver adjusts his/her movement by putting on the accelerating or the braking pedal. This means the controlled variable by the driver is only the acceleration. This property is satisfied in the model (1), (3), and (4). Note that the variables which influence the driver's stimulus are not only the headway. The relative velocity Δv should also be an important variable. Suppose that a driver just merges into an expressway at 60 km/h, and the vehicle in front of him/her is running at 100 km/h, with the headway 15 m. In such a situation, do we need to put on the braking pedal due to the short headway? Instead, we rather accelerate our vehicle to follow the mainstream.

(B) In real driving, if a crash happens, any vehicles must be completely stopped and traffic flow is not able to be established. Thus models, which continue calculations after crashes, are not suitable for traffic simulations. Furthermore, the simulation results after crashes are fabricated and meaningless.

(C) This property is also important when we investigate a car-following model. All the parameters in the model should be clearly measurable by the experimental or observed data for making the model realistic.

III. CAR-FOLLOWING MODEL INCLUDING RELATIVE VELOCITY EFFECTS

Now we propose a different car-following model taking into account the criteria given in Sec. II. We assume that drivers' responses depend on three quantities: their headway, their own velocity, and their relative velocity.

We further suppose that accelerations and decelerations are asymmetric. That is, the braking deceleration is usually stronger than the acceleration because of the strong will of drivers to avoid the crashes. This asymmetry has a significant effect on the time evolutions of the spatial-temporal pattern of traffic jams. We believe that this assumption is natural and our experiment also shows this property (see Sec. VI) [21].

Our new model is described as

$$\frac{d}{dt}v_j = a - b\frac{v_j}{(h_j - d)^2}\exp(-c\Delta v_j) - \gamma v_j, \tag{5}$$

where v_j is the velocity of the jth vehicle, and $h_j = x_{j+1} - x_j$ is the headway to the vehicle in front. The parameter a represents the maximum acceleration in the case $v_j = 0$, and b is the strength of the interaction with the vehicle in front. The other parameters c, d, and γ, which take positive values, respectively represent the weight of the relative velocity effect, the headway when vehicles completely stop, and the strength of the friction or drag. In the case $\Delta v_j < 0$, drivers will decelerate for avoiding a collision with the vehicle in front, and in the opposite case $\Delta v_j > 0$ they accelerate up to their desired velocity.

Figure 1 shows the relation between the relative velocity and the interaction term, i.e., the sum of the first and second terms in the right-hand side of Eq. (5). From this figure the strength of the interaction term is asymmetric with respect to the relative velocity. If the relative velocity is negative, then there is a possibility to crash and drivers try to avoid the accident by strong braking. From the three curves in Fig. 1, we see that the acceleration and the deceleration become stronger when the headway or the velocity is shorter or faster, respectively. The smaller their headway and the larger their velocity, the more strongly drivers put on the brakes because of their avoidance of accidents. Note that these curves are monotonically increasing as Δv_j.

Although Gazis *et al.* considered the relative velocity effect as the linear action to drivers' accelerations as seen in Eq. (1),

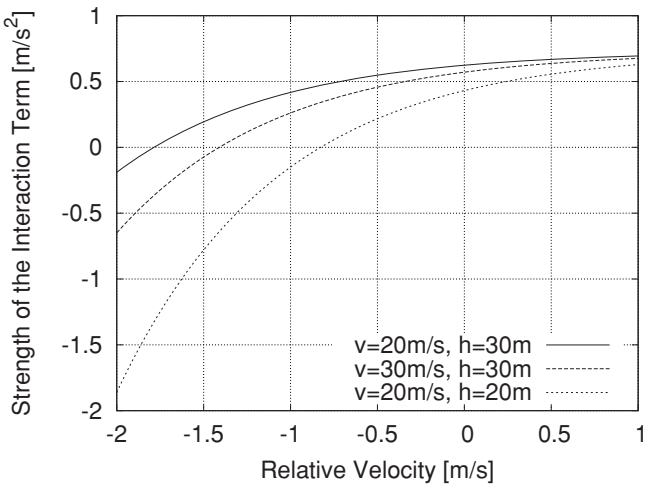

FIG. 1. Curves denoting the relation between the strength of the interaction term $a - bv\exp(-c\Delta v)/(h-d)^2$ and the relative velocity Δv for the parameters $a = 0.73, b = 3.25, c = 1.08, d = 5.25$. The headway and the velocity are smaller and larger, respectively, from top to bottom.

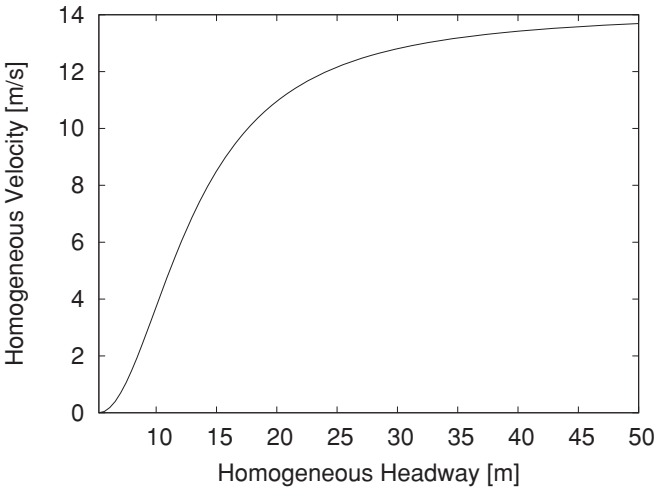

FIG. 2. Relation between the homogeneous headway and the homogeneous velocity for the parameters $a = 0.73, b = 3.25, c = 1.08, d = 5.25, \gamma = 0.0517$. In the limit $h_H \to \infty$, the homogeneous velocity converges to a maximum velocity a/γ.

our model has a nonlinear dependence of it. We can express the driving property in real traffic more efficiently by this improvement, as shown later.

If we set $dv_j/dt = 0$ and $\Delta v_j = 0$ in Eq. (5), our model can naturally lead the relation between the homogeneous headway h_H and the homogeneous velocity v_H, which corresponds to an optimal velocity function introduced in Eq. (2). The homogeneous solution is easily obtained by putting $v_j = v_H$ and $h_j = h_H$ for all j. Then, from Eq. (5) we have

$$v_H = \frac{a(h_H - d)^2}{b + \gamma(h_H - d)^2}. \tag{6}$$

This is illustrated in Fig. 2, which gives the optimal velocity in terms of the headway. We also see that, in the case of the low densities flow $h_j \to \infty$, the homogeneous velocity converges to a/γ.

Note that our model satisfies the criteria of realistic car-following models referred to in Sec. II. First, drivers adjust only their accelerations which depend nonlinearly on their headway, their own velocity, and their relative velocity. Second, in our model, simulations stop due to the divergence of deceleration if h_j becomes d, which corresponds to a crash between the jth vehicle and the $(j+1)$th vehicle. When the headway approaches d, then the braking effect in this model becomes strong due to this singularity. This corresponds to the maneuver that drivers slam their brakes if the inter-vehicular distances between the leading vehicles and their vehicles are approaching to 0. In [17], a similar singularity is introduced, however, the exponent of the singularity is different from our model. The exponent in Eq. (5) is stronger than that of the model in [17]. Note that our model has crashes in numerical simulations although the model has the divergence of deceleration. This is because the time t is discretized and one time step has a finite positive value in numerical simulations. Therefore h_j inevitably becomes less than d under the extreme initial conditions. Finally, our model has just five parameters which are experimentally accessible and it is easy to understand their physical meanings.

In addition, accelerations and decelerations are asymmetric, as seen in Fig. 1. Our model can realize this feature by introducing the exponential function to the interaction term. The strong will for avoidance of the crashes in the case of negative relative velocity is well fit by this function, as shown later.

IV. LINEAR STABILITY ANALYSIS

Let us study the stability of the homogeneous flow $x_j(t) = v_H t + h_H j$, which is one of the exact solutions of Eq. (5). We set the velocity and the headway as

$$v_j(t) = v_H + \alpha_j(t), \tag{7}$$
$$h_j(t) = h_H + \beta_j(t), \tag{8}$$

where α_j and β_j represent small disturbances. Substituting Eqs. (7) and (8) into Eq. (5) and linearizing Eq. (5), the dispersion relation is obtained by putting $\alpha_j = \exp(\mathbf{i}kj + \omega t)$ (the detail calculation is shown in the Appendix). Then this equation for ω is satisfied for two complex roots ω_+ and ω_-:

$$\omega_\pm(k) = \frac{1}{2}\Bigg[-\left(\frac{b}{(h_H-d)^2} + \frac{bcv_H}{(h_H-d)^2}(1-e^{\mathbf{i}k}) + \gamma\right) \pm \sqrt{\left(\frac{b}{(h_H-d)^2} + \frac{bcv_H}{(h_H-d)^2}(1-e^{\mathbf{i}k}) + \gamma\right)^2 - \frac{8bv_H}{(h_H-d)^3}(1-e^{\mathbf{i}k})}\Bigg]. \tag{9}$$

The homogeneous flow is unstable if at least one of the real parts of these solutions is positive. We have verified that the real part of ω_- is always negative for all values of parameters a,b,c,d,γ. This means that the wave described by the dispersion $\omega_-(k)$ will decay exponentially, and disappear very soon. The root ω_- corresponds to the traveling wave going forward, which is sometimes a topic of debate since a forwarding wave is considered to be unphysical in a traffic system [22]. However, this forwarding wave can be understood as an evanescent wave studied in condensed-matter physics or optics [23]. It is a momentary wave that decays exponentially, and can exist only within a short propagating distance in media. Of course in real traffic, perturbations propagate mainly backward because drivers are mostly affected by the vehicles in front. However, a driver sometimes feels psychological pressure from the approaching vehicle from his/her back. This is one of the examples of the momentary forwarding wave in traffic flow. Thus we consider that it is natural for realistic traffic models to have a negative real part of ω in the forward traveling wave.

On the other hand, it is found that the real part of ω_+ can sometimes be positive, which shows the instability of the backward traveling wave. This is shown on the h_H-k plane in Fig. 3.

Let us focus the stability of the backward wave in the limit $k \to 0$. In this case we expand ω_+ in terms of k as

$$\omega_+(k) = \left.\frac{\partial \omega_+}{\partial k}\right|_{k=0} k + \frac{1}{2!}\left.\frac{\partial^2 \omega_+}{\partial k^2}\right|_{k=0} k^2 + \cdots, \tag{10}$$

where

$$\left.\frac{\partial \omega_+}{\partial k}\right|_{k=0} = \mathbf{i}\frac{2bv_H^2}{a(h_H-d)^3}, \tag{11}$$

$$\left.\frac{\partial^2 \omega_+}{\partial k^2}\right|_{k=0} = \frac{2bv_H^2}{a^3(h_H-d)^6}\left[4bv_H^3 - 2abc(h_H-d)v_H^2 - a^2(h_H-d)^3\right]. \tag{12}$$

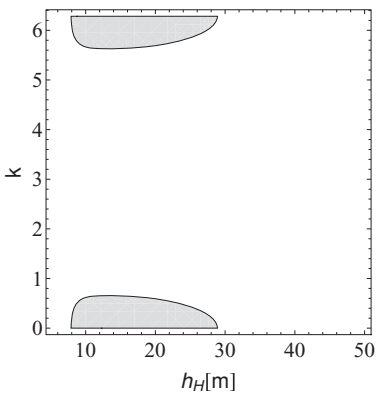

FIG. 3. The instability regions (positive ω_+) of the new car-following model are shown by the shaded areas for the parameters $a = 0.73, b = 3.25, c = 1.08, d = 5.25, \gamma = 0.0517$. The horizontal axis and the vertical axis correspond to the homogeneous headway and the wave number, respectively.

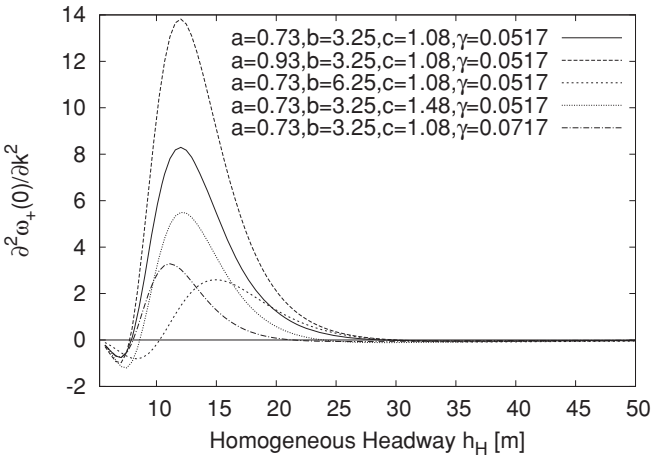

FIG. 4. The relation between the $\partial^2\omega_+(0)/\partial k^2$ and parameters a,b,c,γ. The range of the homogeneous headway is depicted from $h_H = d = 5.25$ to 50 m. In the case $\partial^2\omega_+(0)/\partial k^2 > 0$, the homogeneous flow is unstable in the limit $k \to 0$.

Here $\partial\omega_+(0)/\partial k$ and $\partial^2\omega_+(0)/\partial k^2$ determine the group velocity and the stability of the linearized wave in the region $k \to 0$, respectively. In the case $\partial^2\omega_+(0)/\partial k^2 > 0$, the homogeneous flow is no longer stable. Therefore we have obtained the instability condition in the limit $k \to 0$ as

$$4bv_H^3 - 2abc(h_H-d)v_H^2 - a^2(h_H-d)^3 > 0, \tag{13}$$

where the relation of v_H and h_H is given by Eq. (6). We have understood by Eq. (13) that the homogeneous flow becomes unstable when the homogeneous headway h_H is about from 7.91 to 28.91 m for the parameters $a = 0.73, b = 3.25, c = 1.08, d = 5.25, \gamma = 0.0517$ (see Fig. 3). We use these values of parameters a,b,c,d,γ in the following, which are estimated by the experiment explained in Sec. VI. In this unstable region, drivers' stimuli get to grow as a perturbation propagates backward. Note that the traffic flow becomes stable if the homogeneous headway h_H is lower than 7.91 m. This phenomenon is also seen in model (3).

Next, let us investigate the relation between the instability and the parameters a,b,c,γ in detail. Figure 4 shows that the unstable regions $\partial^2\omega_+(0)/\partial k^2 > 0$ get to narrow with increasing value of the parameters b,c,γ. However, the increase of the parameter a makes the system more unstable. We have also obtained the critical line of the instability on the b-h_H plane. The region surrounded by the critical line in Fig. 5 is unstable. We can immediately check that the critical line is connected on the b-h_H plane and the instability regions get smaller as the parameters c,γ are taking more larger values. Figure 6 shows the instability on the c-h_H plane. From the figures, increasing the value of the parameters b and γ generally results in the improvement of stability of traffic flow. This is due to the improvement of the sensitivity of the drivers. However, it is interesting to see that, in the case $c < 1.3$, increasing the strength of the interaction b makes the system more unstable when h_H is larger than 26 m.

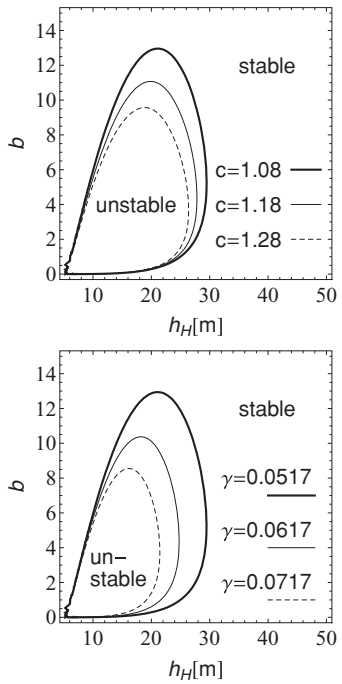

FIG. 5. The critical lines of the instability on b-h_H plane in the case $k \to 0$. The range of the homogeneous headway is depicted from $h_H = d = 5.25$ to 50 m. The upper figure shows the change of the critical line in terms of the parameter c. The thick, thin, and dashed lines correspond to $c = 1.08, 1.18, 1.28$, respectively. The lower figure shows the similar change of the critical line against the parameter γ. The other parameters are the same as in Fig. 3. In both figures, the inside region surrounded by the critical line is unstable.

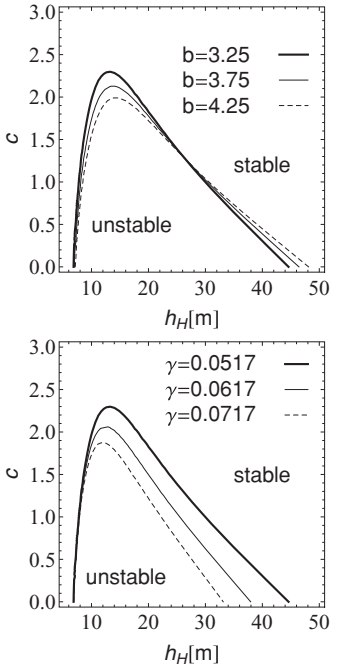

FIG. 6. The critical lines of the instability on c-h_H plane in the case $k \to 0$. The range of the homogeneous headway is depicted from $h_H = d = 5.25$ to 50 m. The upper figure shows the change of the critical line against the parameter b. The lower figure shows the change of the critical line against the parameter γ. The other parameters are the same as in Fig. 3.

V. SIMULATION

In this section, we perform simulations under the periodic boundary condition to investigate the behavior of model (5). Simulations start with the condition that all the vehicles take the same velocity and the same headway expressed by Eq. (6). A small perturbation to the velocity is added to a single vehicle at the beginning of the simulations. We employ the fourth-order Runge-Kutta method for the time update.

Note that as for the simulations of the new model there are no crashes on one-lane periodic roads if a crash does not occur in the beginning. In addition, since the time t is discretized in numerical simulations, crashes inevitably happen only when we set the extreme initial conditions, such as the case that the headway of the following vehicle is very small and its velocity is much larger than the velocity of the vehicle in front of it.

Now let us present typical results of traffic congestion in Fig. 7. This shows a space-time plot which denotes the traces of individual vehicles. A disturbance starts to grow and a cluster of congestion, which propagate in the opposite direction to the movement of vehicles, emerges. The velocity plots of each vehicle at $t = 0.0$, 100.0, 1700.0 sec are given in Fig. 8 (upper). The cluster of congestion at $t = 1700.0$ sec, which is numerically confirmed to be a stationary state, has an asymmetrical feature. Namely, the upstream boundary of the cluster is narrower than the downstream side. This means that drivers are more sensitive to the rapid decrease of the vehicle's velocity than the increase. We can also confirm this asymmetry by the Fig. 8 (lower), which is the plot of the time evolution of density, i.e., inverse of headway.

Figure 9 shows the relation between the flux q and the average density $\bar{\rho}$, which is called the fundamental diagram.

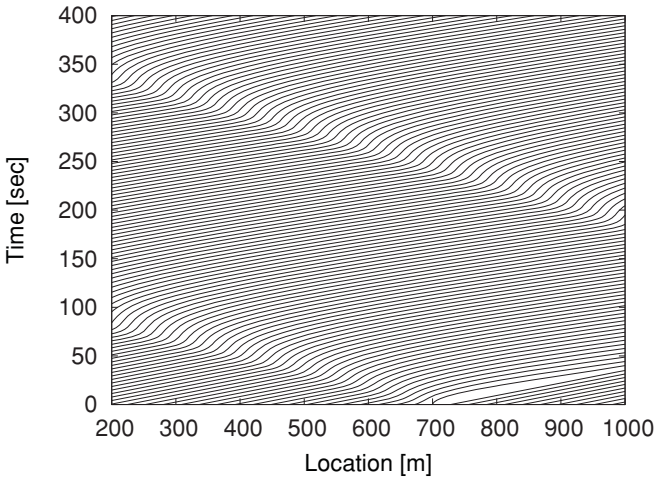

FIG. 7. A space-time plot of vehicles' trajectories. The horizontal axis denotes the positions of vehicles and the vertical axis denotes the time. The number of the total vehicles in the circuit are 100, and the length of the circuit is 1400 m (trajectories are depicted every two vehicles). The initial condition is set for $v_1 = 0.0$, $v_j = v_H$ $(j > 1)$, $h_j = h_H$. The other parameters are the same as in Fig. 3.

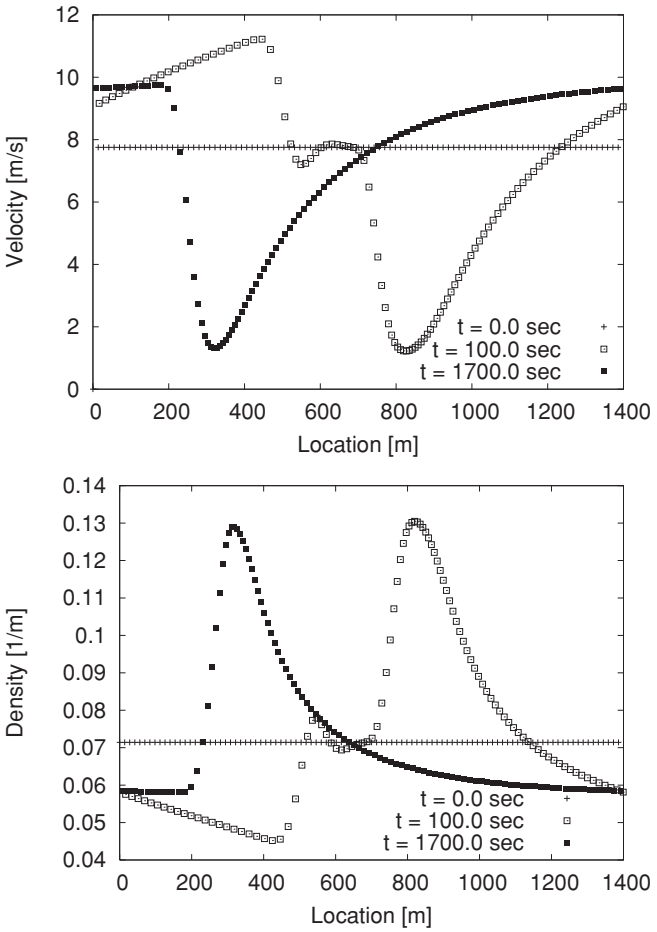

FIG. 8. Vehicles' velocities (upper) and inverse of headway (lower) versus location of each vehicle are plotted at $t = 0.0, 100.0, 1700.0$sec. The length of the circuit is 1400 m and the total vehicles in the circuit are 100. The initial condition is set for $v_1 = 0.0$, $v_j = v_H$ $(j > 1)$, $h_j = h_H$. The horizontal axis denotes the locations of vehicles. The vertical axis denotes the velocities of vehicles (upper) and inverse of headway (lower). The other parameters are the same as in Fig. 3.

The flux of the homogeneous flow is obtained as

$$q = \bar{\rho} v_H, \tag{14}$$

where $\bar{\rho}$ is the average density given by dividing the circuit length by the total number of vehicles in the circuit. The homogeneous velocity v_H is given by Eq. (6). The range of $\bar{\rho} > 0.190 = 1/5.25$ corresponds to the situation $h < d = 5.25$. In the range of the average density from 0.035 to 0.126/m, the fluxes of simulations are lower than those of the homogeneous flow due to the emergence of traffic congestion. This means that the homogeneous flow becomes unstable in this region, and easily changes into a jamming flow by a small perturbation. The upper branch of two curves in the region 0.035 to 0.126/m is called the metastable state.

In Fig. 8, we see clearly the coexistence of the stationary jamming cluster and free flow in a circuit. The two states are plotted in Fig. 9, which are indicated by points F and J. Note that the clusters propagate as solitary waves and maintain their

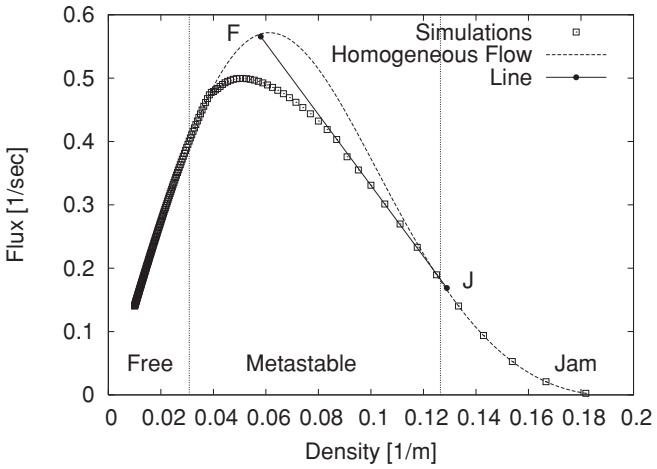

FIG. 9. The relation between the flux and the average density. Data points are obtained by averaging after the relaxation. The flux of the homogeneous flow is calculated by (14). The line F-J is obtained by the simulation given in Fig. 8. The parameters a, b, c, d, γ are the same as in Fig. 3.

size and velocity. The velocity of the cluster v_B can be obtained by the following equation:

$$v_B = \frac{\rho_J v_J - \rho_F v_F}{\rho_J - \rho_F}, \tag{15}$$

where ρ_F (ρ_J) is the density of free (jam) flow in the circuit, and v_F (v_J) is the velocity that corresponds to ρ_F (ρ_J), respectively. In Fig. 9, the velocity of the cluster v_B is represented by the tangent of the line and points F and J denote $(\rho_F, \rho_F v_F)$ and $(\rho_J, \rho_J v_J)$, respectively. Here the density is defined as the inverse of the headway. (ρ_F, v_F) and (ρ_J, v_J) are (0.0581, 9.74) and (0.1289, 1.31), respectively, from the numerical data. Therefore we obtain the velocity of the cluster v_B as -5.60 m/s, which corresponds to -20.2 km/h. This is in good agreement with observed data [24].

It should be noted that the rarefaction shock wave exists in our model, although it cannot exist in usual fluid since it breaks the law of entropy [25]. Vehicles are self-driven particles, not the Newtonian particles, thus the the law of entropy cannot be applied directly to the motion of vehicles. The rarefaction shock wave is an expansion wave that maintains its profile during the propagation. The density of its upstream area is higher than that of the downstream area, and it propagates to the opposite direction of the vehicles. If there is an inflection point on the curve in the fundamental diagram, then we can prove the existence of the rarefaction shock wave [26]. From the result of simulations plotted in Fig. 9, the inflection point is around 0.12/m.

VI. EXPERIMENT

In order to verify the relative velocity effect, we conducted an experiment by using an oval course given in Fig. 10. We use 12 vehicles for this experiment, and give an instruction to the drivers that they should keep constant velocity of 30 km/h and their headway if there is enough free space ahead of them. The three types of homogeneous flow are chosen for initial conditions, i.e., the headway 8, 10, and 15 m with the velocity

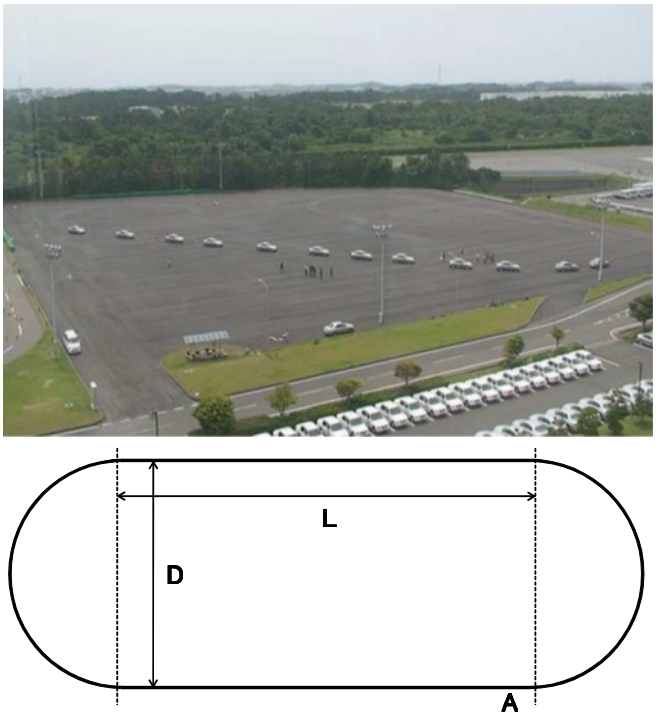

FIG. 10. (Color online) The snapshot and the sketch of the circuit of our experiment. The conditions are $L = 100$ m, $D = 50$ m.

30 km/h. After observing stable flow, the driver of the leading vehicle is told to put on the braking pedal at point A indicated in Fig. 10 to decelerate his vehicle. We set two types of braking: soft braking and hard braking. For soft (hard) braking, the velocity of the leading vehicle decreases from 30 km/h to 25 (20) km/h. Then in these six cases various perturbation waves of the deceleration propagate backward. We study these waves by getting the data of the velocity, the headway, and the acceleration of each vehicle using GPS devices.

In order to investigate the relation between the relative velocity and the acceleration, we have to fix the other physical values. Therefore we focus on the sectional data, which are extracted from the total data under the condition that the velocity and the headway regions are from 25 to 35 km/h and from 14 to 19 m. Then we employed the average value $\bar{v}$ and $\bar{h}$ of the extracted data as the representative values. Specifically, we obtained the values of $\bar{v}$ and $\bar{h}$ as 8.484 m/s and 15.52 m, respectively.

The relation between the acceleration and the relative velocity is shown in Fig. 11. Obviously, the acceleration is positively correlated with the relative velocity. In the case $\Delta v > 0$, the acceleration tends to take a positive value. On the other hand, the acceleration tends to take a negative value in the counter case. However, in the neighborhood of the origin, there are some plots in which the acceleration takes a positive value in spite of the relative velocity taking a negative value. This is because drivers do not have to put on the brake immediately due to the small deceleration of the vehicle in front and enough headway. Figure 11 also shows the difference of the strength between the acceleration and the deceleration. That is, the deceleration resulting from putting on the brake is stronger than the acceleration resulting from putting on the accelerator.

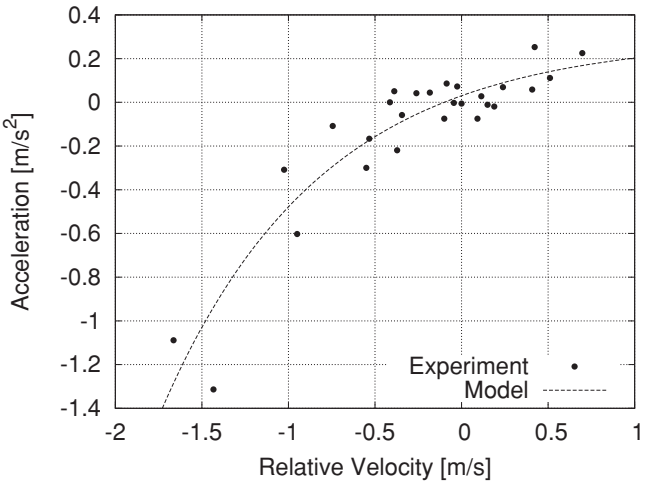

FIG. 11. This is the graph of the relation between the relative velocity and the acceleration. Points are the experimental data, which are extracted under the condition that the velocity and the headway regions are from 25 to 35 km/h and from 14 to 19 m, respectively. The dashed line is $a - b\bar{v}\exp(-c\Delta v)/(\bar{h} - d)^2 - \gamma\bar{v}$, where $\bar{v}$, $\bar{h}$ are the average values of the extracted experiment data: $\bar{v} = 30.54$ km/h $= 8.484$ m/s, $\bar{h} = 15.52$ m. The other parameters are the same as in Fig. 3.

Drivers tend to put on the brake more strongly because drivers want to avoid the crush. We have shown clearly in Fig. 11 that our exponential function fits quite well to the relation between the acceleration and the relative velocity. From the experimental data, we have confirmed that the acceleration has the positive correlation with the relative velocity; there is a asymmetry between the acceleration and the deceleration and the exponential function represents the relation between the acceleration and the relative velocity. Note that the exponential curve of the acceleration demonstrates for low-speed traffic. It is because the experiment is conducted on a short circuit.

Finally, we show the estimated values of parameters a,b,c,d,γ in Table I. We have employed a maximum acceleration of normal vehicles and normal drivers as the value of the parameter a [14]. The parameter d is estimated from the experiment by investigating the headway at which drivers have to stop. The desired velocity estimated by the circuit experiment is about 14.1 m/s (corresponding to 50.8 km/h). It takes a small value because the experiment is conducted on a short circuit. Of course the new model can be also adopted to high-speed traffic, such as the expressway traffic, by recalibration.

TABLE I. The parameters estimated by the circuit experiment.

Parameters	Estimated values
a	0.73
b	3.25
c	1.08
d	5.25
γ	0.0517

VII. CONCLUDING DISCUSSIONS

In this paper, we have proposed criteria of realistic car-following models and have formulated a new car-following model satisfying the criteria. The models have the asymmetry between accelerations and decelerations and the singularity of the vehicle's crash. By analyzing the linear stability, it is confirmed that it has the instability of the homogeneous flow. We have verified the relative velocity effect by investigating experimental data, and have estimated the values of parameters. Experimental data have shown that the acceleration is positively correlated with the relative velocity. Furthermore, it is also shown that the exponential function fits well with the observed data taken from the experiments. Moreover, the parameters in the model are all estimated by the data, and the backward velocity of jam cluster in this model shows 20.2 km/h, which agrees with real traffic data.

We are currently investigating further mathematical properties of this model, including the size and number of asymptotic clusters depending on initial conditions. The results will soon be published elsewhere.

In our model, in the case that the inter-vehicular distance is close to 0, the deceleration takes a larger value than what is physically possible because of the equipment of the singularity. For practical uses, it is one of the possible ways to cut off the deceleration with some threshold around -12 m/s, which is measured on dry road. Improvement of the model for practical uses is under study.

Additionally, the detailed analysis of the crash is also our future work. The study dealing in this analysis such as [27] is significant for considering traffic flow with accidents. Then it is important to know the relation between the acceleration and the short headway, which is out of the scope in our modeling as well as our experiments. Therefore we will get more experimental data to examine the singularity in our model in detail.

Moreover, model (5) is not equipped with explicit time delay or the time derivate of the acceleration [28] for analytical simplicity. It does not make a significant difference to introduce the time delay in the acceleration term if it is small [29]. However, there exist some studies which include time delay [30] and some studies investigated the relation between the time delay and instability in respect to global bifurcation [31,32]. The extension to a model with time delay is also our future work.

APPENDIX: CALCULATION OF LINEAR STABILITY ANALYSIS

In this Appendix, we show the detail of how the dispersion relation (A2) is obtained. Substituting Eqs. (7) and (8) into Eq. (5), we have obtained the following equation for α after linearization:

$$\ddot{\alpha_j} = \frac{2bv_H}{(h_H-d)^3}(\alpha_{j+1}-\alpha_j) - \frac{b}{(h_H-d)^2}\dot{\alpha_j} + \frac{bcv_H}{(h_H-d)^2}(\dot{\alpha_{j+1}}-\dot{\alpha_j}) - \gamma\dot{\alpha_j}, \tag{A1}$$

where $\dot{\alpha_j} = d\alpha_j/dt, \ddot{\alpha_j} = d^2\alpha_j/dt^2$. By putting $\alpha_j = \exp(\mathbf{i}kj + \omega t)$, the dispersion relation is obtained as

$$\omega^2 + \left(\frac{b}{(h_H-d)^2} + \frac{bcv_H}{(h_H-d)^2}(1-e^{\mathbf{i}k}) + \gamma\right)\omega + \frac{2bv_H}{(h_H-d)^3}(1-e^{\mathbf{i}k}) = 0, \tag{A2}$$

where k is the wave number, ω is the frequency, and $\mathbf{i}$ is the imaginary unit.

[1] D. Chowdhury, L. Santen, and A. Schadschneider, Phys. Rep. **329**, 199 (2000).
[2] D. Helbing, Rev. Mod. Phys. **73**, 1067 (2001).
[3] G. M. Schütz, *Phase Transitions and Critical Phenomena* (Academic, New York, 2001), Vol. 19.
[4] H. J. Payne, in *Mathematical Models of Public Systems*, Simulation Council Proceedings, edited by G. A. Bekey (Simulation Council, La Jolla, CA, 1971), Vol. 1, p. 51.
[5] B. S. Kerner, *The Physics of Traffic* (Springer, Heidelberg, 2004).
[6] Y. Sugiyama, M. Fukui, M. Kikuchi, K. Hasebe, A. Nakayama, K. Nishinari, S. Tadaki, and S. Yukawa, New J. Phys. **10**, 033001 (2008).
[7] D. C. Gazis, R. Herman, and R. B. Potts, Oper. Res. **7**, 499 (1959).
[8] D. C. Gazis, R. Herman, and R. W. Rothery, Oper. Res. **9**, 545 (1961).
[9] G. F. Newell, Oper. Res. **9**, 209 (1961).
[10] W. Helly, in *Proceedings of the Symposium on Theory of Traffic Flow*, edited by R. C. Herman (Elsevier, New York, 1959), p. 207.
[11] M. Brackstone and M. McDonald, Transport. Res. F-Traf. **2**, 181 (1999).
[12] M. Bando, K. Hasebe, A. Nakayama, A. Shibata, and Y. Sugiyama, Phys. Rev. E **51**, 1035 (1995).
[13] Y. Sugiyama, Comput. Phys. Commun. **121-122**, 399 (1999).
[14] M. Treiber, A. Hennecke, and D. Helbing, Phys. Rev. E **62**, 1805 (2000).
[15] T. Apeltauer, P. Holcner, M. Kysely, and J. Macur, Silnicni Obzor. **3**, 65 (2007).
[16] R. Jiang, Q. Wu, and Z. Zhu, Phys. Rev. E **64**, 017101 (2001).
[17] E. Tomer, L. Safonov, and S. Havlin, Phys. Rev. Lett. **84**, 382 (2000).
[18] K. Nagel, P. Wagner, and R. Woesler, Oper. Res. **51**, 681 (2003).
[19] I. Lubashevsky, P. Wagner, and R. Mahnke, Phys. Rev. E **68**, 056109 (2003).
[20] P. Ranjitkar, T. Nakatsuji, Y. Azuta, and G. S. Gurusinghe, Transport. Res. Rec. **1852**, 140 (2003).
[21] However, some researchers state that acceleration and deceleration are symmetric and there are some data indicating this symmetry, such as [20]. Bear in mind that this contradicting opinion is also supported by some researchers..
[22] C. Daganzo, Transport. Res. B-Meth. **29**, 277 (1995).

[23] F. de Fornel, *Evanescent Waves From Newtonian Optics to Atomic Optics*, edited by W. T. Rhodes (Springer, London, 2001).
[24] B. S. Kerner and H. Rehborn, Phys. Rev. E **53**, R1297 (1996).
[25] J. D. Anderson, *Modern Compressible Flow* (McGraw-Hill, New York, 1989).
[26] G. B. Whitham, *Linear and Nonlinear Waves* (Wiley Interscience, London, 1974).
[27] W. Xin, J. Hourdos, P. Michalopoulos, and G. Davis, Transport. Res. Rec. **2088**, 126 (2008).
[28] I. Lubashevsky, P. Wagner, and R. Mahnke, Eur. Phys. J. B **32**, 243 (2003).
[29] M. Bando, K. Hasebe, K. Nakanishi, and A. Nakayama, Phys. Rev. E **58**, 5429 (1998).
[30] P. G. Gipps, Transport. Res. B-Meth. **15B**, 105 (1981).
[31] G. Orosz, R. E. Wilson, and B. Krauskopf, Phys. Rev. E **70**, 026207 (2004).
[32] G. Orosz, R. E. Wilson, R. Szalai, and G. Stepan, Phys. Rev. E **80**, 046205 (2009).